for variables, with $P < 0.05$ in the univariate analyses. Only patients with solitary tumours treated with curative resection were included in the survival analysis. Patients who died of diseases other than HCC or liver failure were excluded from the overall survival analysis. Results were deemed statistically significant if $P < 0.05$. Data analysis was conducted with Dr SPSS version II (SPSS, Inc., Tokyo, Japan) and EZR (Saitama Medical Center, Jichi Medical University, Saitama, Japan), a graphical user interface for R (the R Foundation for Statistical Computing, Vienna, Austria).

ETHICS

The Ethics Committee of the University of Tokyo approved the study.

Results

PATIENT CHARACTERISTICS

There were 293 patients with a total of 382 HCC tumours that met the inclusion criteria of the study. During this study period, about 1500 HCCs were treated with 650 surgical procedures, including conventional hepatectomies and transplants. The mean age of the patients was 65 years (range 19–83 years). There were 229 male and 64 female patients. Fifty-four patients (18.4%) were HBV(+)/HCV(−), 138 (47.1%) were HBV(−)/HCV(+), two (0.7%) were HBV(+)/HCV(+) and 99 (33.8%) were HBV(−)/HCV(−). Diabetes mellitus was documented in 111 patients (37.9%), hypertension in 124 (42.3%) and hyperlipidaemia in 14 (4.8%). Sixty-seven (22.9%) had a BMI of 25 or greater. There were 112 patients (38.2%) with a history of alcohol intake (20 g or more per day for at least 1 year) and 29 (9.9%) with a history of heavy drinking (80 g or more per day for at least 5 years). Other chronic liver or biliary diseases were not documented in any of the patients.

CLINICOPATHOLOGICAL CHARACTERISTICS OF SH-HCC

There were 120 HCCs (31.4%) in 106 patients (36.3%) that met the criteria for SH-HCC, including 54 HCCs (14.1%) in 51 patients (17.5%) corresponding to typical SH-HCC.

Sixty-two patients had multiple HCCs. Among them, 32 had only conventional HCCs (C-HCCs), 23 had both C-HCCs and SH-HCCs, and seven had only SH-HCCs. One patient had C-HCC and intrahepatic cholangiocarcinoma (ICC), one had C-HCC and combined HCC-ICC, one had three SH-HCCs and one ICC, and one had two C-HCCs and one combined HCC-ICC.

Table 1 shows the characteristics of patients with SH-HCC, with or without C-HCC. Compared to patients with only C-HCC, patients with SH-HCC had a relatively higher frequency of female sex, non-viral aetiology, diabetes mellitus and hypertension, and a lower frequency of a history of alcoholic intake ($P < 0.05$). Serologically, patients with SH-HCC were characterized by a higher level of total cholesterol and triglycerides and a lower level of alpha-fetoprotein ($P < 0.05$). Cirrhosis was observed with similar frequencies in the SH-HCC and C-HCC groups. The background liver of SH-HCC patients were more frequently steatotic ($P = 0.0004$), although the degree of steatosis was generally mild (grade 1, 89%; grade 2, 9%; grade 3, 2%). Features suggestive of steatohepatitis, including typical hepatocellular ballooning, zone 3 fibrosis or Mallory–Denk bodies, were observed more frequently ($P < 0.0001$). The patients' characteristics of SH-HCC mentioned above applied almost equally to those of typical SH-HCC.

Table 2 shows the incidence of SH-HCC according to aetiology. Of 71 HCCs arising from a HBV(+)/HCV(−) background, 13 (18.3%) were SH-HCC and one (1.4%) was typical SH-HCC, which was significantly lower than the percentage of HCCs from a HBV(−)/HCV(+) (SH-HCC, 30.6%; typical SH-HCC, 14.2%) or HBV(−)/HCV(−) (SH-HCC, 40.7%; typical SH-HCC, 22.0%) background.

SH-HCCs occurred frequently in the context of metabolic conditions. There was a significantly higher proportion of SH-HCC and typical SH-HCC in HCCs with background diabetes mellitus or hypertension than those without ($P < 0.01$). HCCs with background hyperlipidaemia had a non-significantly higher proportion of SH-HCC and typical SH-HCC. In contrast, HCCs arising in patients with a history of alcohol intake had a lower incidence of SH-HCC than those without ($P = 0.0054$). HCCs arising in steatotic livers had a higher proportion of SH-HCC and typical SH-HCC than those in non-steatotic livers ($P < 0.01$). HCCs arising with a background of steatohepatitis showed a much higher proportion of SH-HCC and typical SH-HCC than those without steatohepatitis ($P < 0.0001$).

HISTOLOGICAL CHARACTERISTICS

Histologically, all SH-HCCs showed steatosis, at least focally. Marked (macrovesicular steatosis in ≥67% cells), moderate (34–66%) and mild (5–33%) steatosis

Table 1. Characteristics of patients with steatohepatitic hepatocellular carcinoma

	C-HCC (n = 187)	All SH-HCC (n = 106)	P*	Typical SH-HCC (n = 51)	P†
Age (years, mean ± SD)	64.0 ± 11.8	66.7 ± 10.8	0.0599	68.0 ± 7.9	**0.0236**
Sex (male:female)	153:34	76:30	**0.0439**	34:17	**0.0194**
HBV(+)/HCV(−)	42 (22.5%)	12 (11.3%)	**0.0208**	1 (2.0%)	**0.0003**
HBV(−)/HCV(+)	90 (48.1%)	48 (45.3%)		25 (49.0%)	
HBV(+)/HCV(+)	1(0.5%)	1(0.9%)		0(0.0%)	
HBV(−)/HCV(−)	54 (28.9%)	45 (42.5%)		25 (49.0%)	
Diabetes mellitus (+)	57 (30.5%)	54 (50.9%)	**0.0005**	33 (64.7%)	**<0.0001**
Hypertension (+)	68 (36.4%)	56 (52.8%)	**0.0061**	32 (62.7%)	**0.0007**
Hyperlipidemia (+)	7 (3.7%)	7(6.6%)	0.2700	4 (7.8%)	0.2557
History of alcohol intake (+)‡	80 (42.8%)	32 (30.2%)	**0.0331**	15 (29.4%)	0.0840
History of heavy drinking (+)§	22 (11.8%)	7 (6.6%)	0.1552	4 (7.8%)	0.6129
BMI ≥25 (kg/m^2)	36 (19.3%)	31 (29.2%)	0.0503	15 (29.4%)	0.1170
TP (g/dl, mean ± SD)	7.11 ± 0.53	7.13 ± 0.56	0.8386	7.15 ± 0.58	0.6831
ALB (g/dl, mean±SD)	3.67 ± 0.44	3.72 ± 0.41	0.3352	3.72 ± 0.36	0.4288
ChE (IU/l, mean ± SD)	216.8 ± 74.1	231.6 ± 80.4	0.1109	229.9 ± 80.1	0.2710
LDH (IU/l, mean ± SD)	231.2 ± 69.0	239.3 ± 79.9	0.3622	236.9 ± 54.2	0.5902
AST (IU/l, mean ± SD)	45.3 ± 24.4	51.9 ± 54.3	0.2365	44.0 ± 24.3	0.7294
ALT (IU/l, mean ± SD)	44.5 ± 38.2	43.7 ± 29.4	0.8571	38.9 ± 24.2	0.3205
GGTP (IU/l, mean ± SD)	93.0 ± 105.3	88.4 ± 89.1	0.7059	87.2 ± 95.7	0.7227
ALP (IU/l, mean ± SD)	285.2 ± 202.5	274.5 ± 168.0	0.6458	247.8 ± 92.7	0.2015
TB (mg/dl, mean ± SD)	0.74 ± 0.30	0.76 ± 0.30	0.6627	0.78 ± 0.32	0.4674
T.Cho (mg/dl, mean ± SD)	163.5 ± 35.3	177.6 ± 41.3	**0.0022**	172.5 ± 33.5	0.1054
TG (mg/dl, mean ± SD)	90.2 ± 39.5	111.4 ± 54.4	**0.0005**	113.4 ± 52.7	**0.0046**
PT (%, mean ± SD)	83.6 ± 12.8	84.8 ± 12.9	0.4413	85.8 ± 12.5	0.2953
Plt (×10^4/μl, mean ± SD)	17.6 ± 8.4	18.1 ± 9.4	0.6406	16.6 ± 8.7	0.4773
ICG15 (%, mean ± SD)	14.6 ± 8.5	15.5 ± 9.7	0.3844	16.0 ± 7.9	0.2756
Child-Pugh (A/B)	169/18	99/7	0.3736	48/3	0.5793
AFP (ng/ml, median [IQR])	28.0 (632.5)	11.5 (96.0)	**0.0324**	10.0 (44.9)	**0.0190**
PIVKA2 (mAu/ml, median [IQR])	140.5 (2970.8)	97.0 (715.0)	0.1008	68.0 (266.8)	**0.0487**

Table 1. *(Continued)*

	C-HCC (n = 187)	All SH-HCC (n = 106)	P*	Typical SH-HCC (n = 51)	P†
Preoperative treatment (no/yes)**	113/74	75/31	0.0765	35/16	0.2844
Liver cirrhosis (no/yes)	118/69	66/39¶	0.9670	26/25	0.1165
Steatosis (absent/present)	130/57	51/54¶	**0.0004**	21/30	**0.0003**
Steatosis grade (0/1/2/3)	(130/51/5/1)	(51/48/5/1)	**0.0023**	(21/28/2/0)	**0.0009**
Steatohepatitis (absent/present)	161/26	64/41¶	**<0.0001**	24/27	**<0.0001**

C-HCC, conventional hepatocellular carcinoma; SH-HCC, steatohepatitic hepatocellular carcinoma; HBV, hepatitis B virus; HCV, hepatitis C virus; BMI, body mass index; TP, total protein; ALB, albumin; ChE, cholinesterase; LDH, lactate dehydrogenase; AST, aspartate aminotransferase; ALT, alanine aminotransferase; GGTP, gamma-glutamyl transpeptidase; ALP, alkaline phosphatase; TB, total bilirubin; T.Cho, total cholesterol; TG, triglycerides; PT, prothrombin time; Plt, platelet count; ICG15, indocyanine green retention at 15 min; AFP, alpha-fetoprotein; PIVKA2, protein induced by vitamin K absence or antagonist-II; SD, standard deviation; IQR, interquartile range. Significant P-values are indicated in bold.
*Comparison between C-HCC and all SH-HCC.
†Comparison between C-HCC and typical SH-HCC.
‡Intake of 20 g or more of alcohol per day for at least 1 year.
§Intake of 80 g or more of alcohol per day for more than 5 years.
¶Background liver of one patient could not be assessed.
**Preoperative treatment included transcatheter arterial embolization, transcatheter arterial infusion chemotherapy, transcatheter arterial chemoembolization, or portal embolization.

was noted in 13, 22 and 66 tumours, respectively. In 19 tumours, macrovesicular steatosis was observed only in <5% of tumour cells. Tumour cell ballooning was seen in all SH-HCCs, at least focally. Fibrosis, either of the paratrabecular or internodular types, was observed to varying degrees in 113 of 120 SH-HCCs. Ten SH-HCCs were accompanied by extensive fibrosis, comparable to the degree seen in scirrhous HCC. Intratumoural inflammatory infiltration was observed in 115 cases. Mallory–Denk bodies were found in 113 tumours. For the subset of SH-HCC that met only four of the five criteria, the most frequent missing criterion was steatosis, followed by fibrosis and Mallory–Denk bodies.

Steatosis was frequently more pronounced in SH-HCC than in the background liver tissue. When comparing the extent of steatosis in SH-HCC and in the background liver (3 + , ≥67% of tumour cells or background hepatocytes; 2+, 34–66%; 1+, 5–33%; 0, <5%), 66 SH-HCCs had more, 43 had equivalent and only nine had less steatosis than background liver tissue (data on the background liver was not available for one patient with two SH-HCCs).

SH-HCCs were characterized by smaller size (median, 27.0 mm versus 35.0 mm), a higher frequency of well- to moderately differentiated histology, and a higher frequency of bile duct invasion ($P < 0.05$) (Table 3). Among well- and moderately differentiated HCCs, SH-HCCs showed a significantly higher frequency of vascular invasion than C-HCCs ($P = 0.0019$). Similar trends were seen with typical SH-HCCs. Of note, typical SH-HCCs were much smaller than C-HCCs (22.5 mm versus 35.0 mm), and even smaller than the non-typical SH-HCCs (22.5 mm versus 35.5 mm, $P = 0.0122$). In addition, typical SH-HCCs were exclusively well- to moderately differentiated (100%). Typical SH-HCCs had a significantly higher frequency of bile duct invasion than C-HCCs ($P = 0.0089$). Typical SH-HCCs showed a significantly higher frequency of vascular invasion than well- and moderately differentiated C-HCCs ($P = 0.0289$).

PROGNOSIS

Survival analysis was performed on patients with solitary HCCs (Figure 2). Steatohepatitic features in HCCs did not affect disease-free or overall survival (Figure 2A,B). When typical and other SH-HCCs were assessed separately, patients with typical SH-

Table 2. Incidence of steatohepatitic hepatocellular carcinoma according to etiology

Background	Total number of HCC	Number of SH-HCC (%)	*P*	Number of Typical SH-HCC (%)	*P*
HBV(+)/HCV(−)	71	13 (18.3)[a]	**0.0481**[a versus b]	1 (1.4)[d]	**0.0014**[d versus e]
HBV(−)/HCV(+)	183	56 (30.6)[b]	**0.0014**[a versus c]	26 (14.2)[e]	**<0.0001**[d versus f]
HBV(+)/HCV(+)	5	1 (20.0)	0.0701[b versus c]	0 (0.0)	0.0793[e versus f]
HBV(−)/HCV(−)	123	50 (40.7)[c]		27 (22.0)[f]	
Diabetes mellitus (+)	144	64 (44.4)	**<0.0001**	36 (25.0)	**<0.0001**
Diabetes mellitus (−)	238	56 (23.5)		18 (7.6)	
Hypertension (+)	175	68 (38.9)	**0.0040**	34 (19.4)	**0.0063**
Hypertension (−)	207	52 (25.1)		20 (9.7)	
Hyperlipidemia (+)	20	8 (40.0)	0.3954	5 (25.0)	0.1520
Hyperlipidemia (−)	362	112 (30.9)		49 (13.5)	
BMI ≥25 (kg/m^2)	94	39 (41.5)	**0.0154**	17 (18.1)	0.2056
BMI <25 (kg/m^2)	288	81 (28.1)		37 (12.8)	
Alcohol intake (+)*	144	33 (22.9)	**0.0054**	15 (10.4)	0.1046
Alcohol intake (−)	238	87 (36.6)		39 (16.4)	
Heavy drinking (+)†	40	7 (17.5)	**0.0451**	4 (10.0)	0.6306
Heavy drinking (−)	342	113 (33.0)		50 (14.6)	
Steatosis (+)	155	60 (38.7)	**0.0091**	32 (20.6)	**0.0027**
Steatosis (−)	226	59 (26.1)		22 (9.7)	
Steatohepatitis (+)	94	46 (48.9)	**<0.0001**	29 (30.9)	**<0.0001**
Steatohepatitis (−)	287	73 (25.4)		25 (8.7)	

HBV, hepatitis B virus; HCV, hepatitis C virus; SH-HCC, steatohepatitic hepatocellular carcinoma; BMI, body mass index. Significant *P*-values are indicated in bold.
*Intake of 20 g or more of alcohol per day for at least 1 year.
†Intake of 80 g or more of alcohol per day for more than 5 years.
Superscripts, a–f, represent each value in cells (13(18.3%), etc.).

HCCs had significantly better disease-free survival than patients with other SH-HCCs or C-HCCs (Figure 2C). Neither SH-HCC nor typical SH-HCC, however, was a significant prognostic factor in the multivariate Cox proportional hazards regression model (Table 4).

Discussion

The incidence of SH-HCC in this study cohort was similar to or somewhat higher than those in previous studies from the United States (13.5–35.5%).[4,5,8,9] Such a high prevalence may be partly attributable to the relatively high incidence of metabolic conditions in the study group. The higher prevalence of SH-HCC in the present study compared to the study by Salomao *et al.*, however, is most likely to be related to the distinct diagnostic criteria used in the two studies: we made the diagnosis of SH-HCC when a tumour fulfilled the histological criteria regardless of whether the features were focal or extensive, whereas Salomao *et al.* considered a tumour SH-HCC when SH features were present in at least 50% of the tumour area on representative tissue sections. Association between

Table 3. Histologic characteristics of steatohepatitic hepatocellular carcinoma

	C-HCC (n = 262)	All SH-HCC (n = 120)	P*	Typical SH-HCC (n = 54)	P†
Location (right lobe/left lobe)	185/77	80/40	0.4376	36/18	0.5649
Location (superficial/deep)‡	55/62	24/43	0.1401	12/26	0.0953
Size (mm, median [IQR])	35.0 (42.3)	27.0 (35.0)	**0.0197**	22.5 (20.3)	**0.0008**
Grade (well/mod/por)	64/145/53	30/80/10	**0.0119**	10/44/0	**<0.0001**
Vascular invasion (present/absent), all cases	123/139	69/51	0.0555	29/25	0.3655
Vascular invasion (present/absent), well/mod HCC cases	78/131	61/49	**0.0019**	29/25	**0.0289**
Bile duct invasion (present/absent)	4/258	8/112	**0.0116**	5/49	**0.0089**
Intrahepatic metastasis (present/absent)	51/211	19/101	0.3943	7/47	0.2610

C-HCC, conventional hepatocellular carcinoma; SH-HCC, steatohepatitic hepatocellular carcinoma; IQR, interquartile range; well, well differentiated; mod, moderately differentiated; por, poorly differentiated. Significant P-values are indicated in bold.

*Comparison between C-HCC and all SH-HCC.

†Comparison between C-HCC and typical SH-HCC.

‡Tumours ≤3 cm in diameter were assessed.

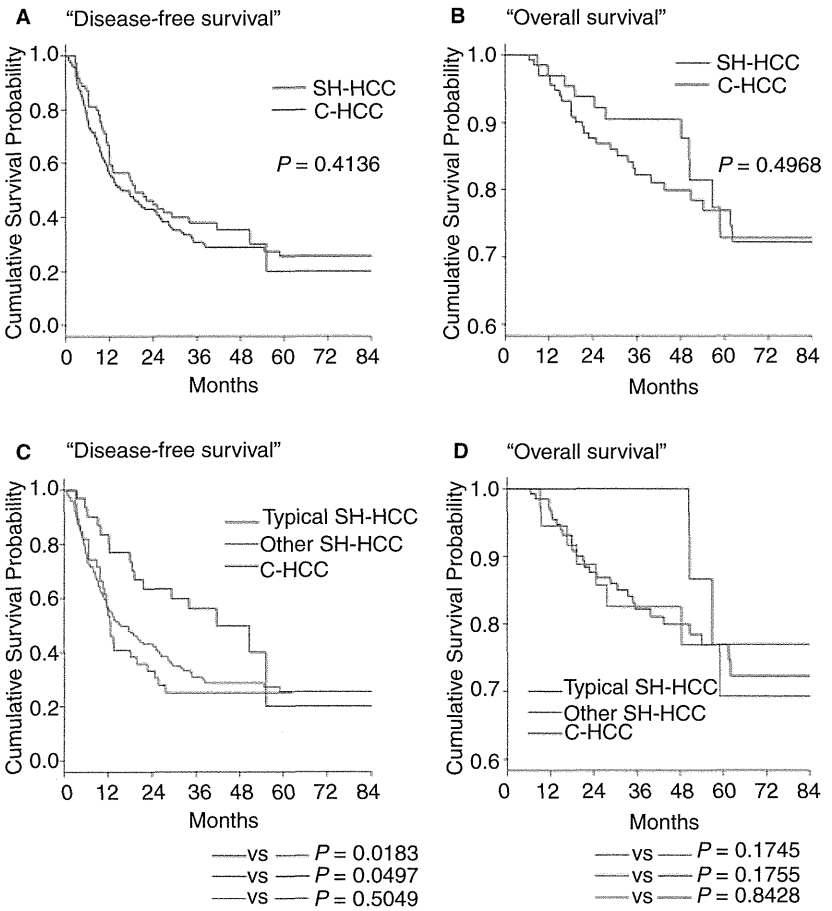

Figure 2. Survival data for solitary hepatocellular carcinoma. Disease-free (**A**) and overall (**B**) survival did not differ between conventional hepatocellular carcinoma (C-HCC) and steatohepatitic hepatocellular carcinoma (SH-HCC). When typical SH-HCC and other SH-HCC were analysed separately (**C**,**D**), typical SH-HCC showed better disease-free survival than other SH-HCC and C-HCC, respectively (**C**).

Table 4. Prognostic factors in solitary HCC

	Disease-free survival				Overall survival			
	Univariate analysis		Multivariate analysis		Univariate analysis		Multivariate analysis	
Factor	HR (95% CI)	*P*	HR (95% CI)	*P*	HR (95% CI)	*P*	HR (95% CI)	*P*
Age (> 65 years versus 0–65 years)	1.179 (0.843–1.647)	0.3356			1.624 (0.834–3.164)	0.1538		
Sex (male versus female)	1.122 (0.762–1.656)	0.5582			1.074 (0.510–2.262)	0.8516		
HBV (positive versus negative)	0.934(0.610–1.430)	0.7539			0.937 (0.414–2.124)	0.8767		
HCV (positive versus negative)	1.149 (0.830–1.589)	0.4030			0.981 (0.523–1.840)	0.9536		
Diabetes mellitus (present versus absent)	0.954 (0.680–1.337)	0.7826			1.667 (0.886–3.136)	0.1132		
Hypertension (present versus absent)	1.014 (0.730–1.409)	0.9332			1.025 (0.541–1.940)	0.9408		
Body mass index (≥25 kg/m^2 versus <25 kg/m^2)	1.023 (0.693–1.508)	0.9102			0.988(0.469–2.082)	0.9748		
History of alcohol intake (present versus absent)	0.915 (0.653–1.283)	0.6069			0.605 (0.301–1.216)	0.1581		
History of heavy drinking (present versus absent)	0.848 (0.458–1.568)	0.5983			0.553 (0.133–2.293)	0.4139		
Child-Pugh (B versus A)	1.573 (0.904–2.737)	0.1091			1.126 (0.346–3.662)	0.8433		
AFP (>20 ng/ml versus 0–20 ng/ml)	1.407 (1.016–1.948)	**0.0400**	1.319 (0.915–1.903)	0.1377	0.866 (0.460–1.631)	0.6560		
Tumour size (>5 cm versus 0–5 cm)	1.932 (1.389–2.687)	**<0.0001**	1.419 (0.972–2.072)	0.0697	2.322 (1.236–4.363)	**0.0088**	1.070 (0.523–2.190)	0.8531
Histologic grade (por versus well/mod)	1.578 (1.069–2.327)	**0.0215**	0.854 (0.535–1363)	0.5083	3.590 (1.859–6.799)	**<0.0001**	2.689 (1.377–5.253)	**0.0038**
SH-HCC (present versus absent)	0.864 (0.609–1.226)	0.4144			0.786 (0.391–1.578)	0.4979		

Table 4. *(Continued)*

	Disease-free survival				Overall survival			
	Univariate analysis		Multivariate analysis		Univariate analysis		Multivariate analysis	
Factor	HR (95% CI)	*P*	HR (95% CI)	*P*	HR (95% CI)	*P*	HR (95% CI)	*P*
Typical SH-HCC (present versus absent)	0.571 (0.339–0.961)	**0.0348**	0.622 (0.363–1.064)	0.0832	0.298 (0.072–1.237)	0.0955		
Vascular invasion (present versus absent)	1.639 (1.162–2.313)	**0.0049**	1.140 (0769–1.690)	0.5146	3.559 (1.570–8.067)	**0.0024**	1.863 (0.749–4.636)	0.1809
Intrahepatic metastasis (present versus absent)	3.453 (2.418–4.932)	**<0.0001**	2.885 (1.915–4.348)	**<0.0001**	4.667 (2.482–8.777)	**<0.0001**	3.253 (1.599–6.619)	**0.0011**
Background liver (LC versus non-LC)	1.421 (1.017–1.986)	**0.0396**	1.515 (1.064–2.156)	**0.0216**	1.343 (0.712–2.532)	0.3622		
Steatosis (present versus absent)	0.874 (0.618–1.235)	0.4448			0.805 (0.413–1.568)	0.5237		
Steatohepatitis (present versus absent)	0.832 (0.554–1.251)	0.3766			0.754 (0.346–1.643)	0.4767		

HR, hazard ratio; CI, confidence interval; HBV, hepatitis B virus; HCV, hepatitis C virus; SH-HCC, steatohepatitic hepatocellular carcinoma; AFP, alpha-fetoprotein; por, poorly differentiated; well, well differentiated; mod, moderately differentiated; LC, liver cirrhosis. Significant *P*-values are indicated in bold.

SH-HCC and metabolic conditions was a cardinal finding in the seminal study by Salomao *et al.*[4] The present study demonstrated a more robust association; unlike the previous study, both diabetes mellitus and hypertension were significantly more prevalent in patients with SH-HCC than those without SH-HCC. In this study cohort only a small number of patients had a history of hyperlipidaemia, but serum levels of total cholesterol and triglycerides were significantly higher in patients with SH-HCC than those with C-HCC. Although we cannot emphasize this result, as the serum data had not been measured under equal nutritional conditions in all the patients, an association between SH-HCC and hyperlipidaemia seems quite plausible, because hyperlipidaemia is a principal feature of the metabolic syndrome.

In line with the high frequency of metabolic conditions in the SH-HCC patients, the background liver of SH-HCC patients more frequently exhibited steatosis. Features suggestive of steatohepatitis were also more prevalent in the SH-HCC group. We do not know the exact frequency of steatohepatitis in our study cohort due to the following reasons. First, it was sometimes difficult to determine the presence of steatohepatitis in patients with chronic viral hepatitis which could, by itself, induce steatosis and hepatocellular ballooning.[10] Secondly, some cases corresponded to cryptogenic cirrhosis which, as is well known, could represent end-stage steatohepatitis.[11] Steatosis was frequently more pronounced in SH-HCC than in the background liver. Therefore, tumour histology tended to be a better indicator of the metabolic background than the background tissue.

When compared to HBV-related HCCs, HCV-related HCCs showed a much higher proportion of SH-HCCs. The difference is partly attributable to the different prevalence of metabolic conditions; diabetes mellitus was significantly more common in HCV-positive patients. Of note, several studies have shown that HCV infection, usually genotype 1, induces insulin resistance and the metabolic syndrome.[12,13] Moreover, a number of studies have shown that HCV infection directly induces steatosis in hepatocytes. This phenomenon results from a cytopathic effect of HCV, associated mainly with genotype 3.[14] Further studies are needed to elucidate whether HCV has a similar cytopathic effect on neoplastic hepatocytes.

One interesting result was the lower frequency of a history of alcoholic intake in the SH-HCC group than in the C-HCC group. We surmise that this result is related to the protective effect of alcohol in fat metabolism. On one hand, alcohol consumption is a well-established causative agent for inducing steatosis or steatohepatitis.[15] On the other hand, recent studies have shown repeatedly that modest alcohol intake has an inverse association with liver fat content or the development of steatohepatitis in NAFLD.[16–18]

The notable histological characteristics of SH-HCCs include a tendency towards invasion, as was shown by a high frequency of vascular and bile duct involvement. We failed to demonstrate prognostic significance of SH-HCC despite such a high frequency of vascular involvement. We infer that this results from the relatively smaller size of SH-HCCs. A recent study showed that microvascular invasion by HCC, the precise prognostic significance of which remains a matter of discussion,[19] was not a prognostic factor in small HCCs.[20]

In this study, we analysed 'typical' SH-HCCs separately, because the relevant histological criteria of SH-HCC were not known at the start of the study and we hypothesized that 'typical' SH-HCC would at least represent this subset. Typical SH-HCCs shared similar characteristics with SH-HCCs in general. Interestingly, they were even smaller than other SH-HCCs and were exclusively well- to moderately differentiated. These findings suggest that typical SH-HCCs represent early-stage SH-HCCs and they possibly lose some steatohepatitic features with tumour progression. Alternatively, C-HCCs can take on steatohepatitic features as they progress. The slightly better prognosis associated with typical SH-HCC probably reflects a smaller size and relatively well-differentiated histology.

Further study is still necessary to characterize SH-HCC more clearly. Unlike the results presented by Salomao *et al.*,[5] a steatohepatitic background does not seem to be the sole determinant of steatohepatitic histology of HCC based on the present study, in which a number of SH-HCC patients lacked background steatohepatitis or metabolic conditions. A similar conclusion was reached by a recent study.[9] It is, therefore, of paramount importance to investigate genetic alterations of SH-HCCs and to identify molecular mechanisms leading to steatohepatitic histology. With some distinct genetic characteristics or association with some genetic subsets of HCCs, SH-HCCs would still be a noteworthy subtype. Morphological characteristics of precursor lesions of SH-HCCs should also be investigated in future studies.

In conclusion, we confirmed that SH-HCCs were a subset of HCCs associated with metabolic conditions and the presence of steatosis or steatohepatitis in the background liver. Although SH-HCC showed invasive characteristics on histology, steatohepatitic features did not represent a significant prognostic factor. Fur-

ther studies, especially on genetic aspects, are necessary to determine the significance of SH-HCC.

Conflict of interests

The authors declare that they have no potential or actual conflicts of interest.

References

1. Ferlay J, Shin HR, Bray F *et al.* Estimates of worldwide burden of cancer in 2008: GLOBOCAN 2008. *Int. J. Cancer* 2010; **127**; 2893–2917.
2. Theise ND, Curado MP, Franceschi S *et al.* Hepatocellular carcinoma. In Bosman FT, Carneiro F, Hruban RH, Theise ND eds. *WHO classification of tumours of the digestive system.* Lyon: IARC, 2010; 205–216.
3. Hoshida Y, Moeini A, Alsinet C *et al.* Gene signatures in the management of hepatocellular carcinoma. *Semin. Oncol.* 2012; **39**; 473–485.
4. Salomao M, Yu WM, Brown RS *et al.* Steatohepatitic hepatocellular carcinoma (SH-HCC): a distinctive histological variant of HCC in hepatitis C virus-related cirrhosis with associated NAFLD/NASH. *Am. J. Surg. Pathol.* 2010; **34**; 1630–1636.
5. Salomao M, Remotti H, Vaughan R *et al.* The steatohepatitic variant of hepatocellular carcinoma and its association with underlying steatohepatitis. *Hum. Pathol.* 2012; **43**; 737–746.
6. Bedossa P, Poynard T. An algorithm for the grading of activity in chronic hepatitis C. The METAVIR Cooperative Study Group. *Hepatology* 1996; **24**; 289–293.
7. Kleiner DE, Brunt EM, Van Natta M *et al.* Design and validation of a histological scoring system for nonalcoholic fatty liver disease. *Hepatology* 2005; **41**; 1313–1321.
8. Busler JF, Geevarghese SK, Kelly BS *et al.* The steatohepatitic variant of hepatocellular carcinoma is associated with nonalcoholic steatohepatitis. *Mod. Pathol.* 2012; **25** (Suppl. S1); 411A.
9. Alexander J, Torbenson M, Wu TT *et al.* Steatohepatitic hepatocellular carcinoma did not increase in the last decade: metabolic syndrome may not be the only contributing factor. *Mod. Pathol.* 2013; **26** (Suppl. S1); 397A.
10. Ishak KG. Pathologic features of chronic hepatitis. A review and update. *Am. J. Clin. Pathol.* 2000; **113**; 40–55.
11. Caldwell SH, Lee VD, Kleiner DE *et al.* NASH and cryptogenic cirrhosis: a histological analysis. *Ann. Hepatol.* 2009; **8**; 346–352.
12. Fartoux L, Poujol-Robert A, Guéchot J *et al.* Insulin resistance is a cause of steatosis and fibrosis progression in chronic hepatitis C. *Gut* 2005; **54**; 1003–1008.
13. Hézode C, Roudot-Thoraval F, Zafrani ES *et al.* Different mechanisms of steatosis in hepatitis C virus genotypes 1 and 3 infections. *J. Viral Hepatol.* 2004; **11**; 455–458.
14. Kumar D, Farrell GC, Fung C *et al.* Hepatitis C virus genotype 3 is cytopathic to hepatocytes: reversal of hepatic steatosis after sustained therapeutic response. *Hepatology* 2002; **36**; 1266–1272.
15. Gao B, Bataller R. Alcoholic liver disease: pathogenesis and new therapeutic targets. *Gastroenterology* 2011; **141**; 1572–1585.
16. Dixon JB, Bhathal PS, O'Brien PE. Nonalcoholic fatty liver disease: predictors of nonalcoholic steatohepatitis and liver fibrosis in the severely obese. *Gastroenterology* 2001; **121**; 91–100.
17. Dunn W, Sanyal AJ, Brunt EM *et al.* Modest alcohol consumption is associated with decreased prevalence of steatohepatitis in patients with non-alcoholic fatty liver disease (NAFLD). *J. Hepatol.* 2012; **57**; 384–391.
18. Gunji T, Sato H, Iijima K *et al.* Modest alcohol consumption has an inverse association with liver fat content. *Hepatogastroenterology* 2012; **59**; 2552–2556.
19. Rodríguez-Perálvarez M, Luong TV, Andreana L *et al.* A systematic review of microvascular invasion in hepatocellular carcinoma: diagnostic and prognostic variability. *Ann. Surg. Oncol.* 2013; **20**; 325–339.
20. Shindoh J, Andreou A, Aloia TA *et al.* Microvascular invasion does not predict long-term survival in hepatocellular carcinoma up to 2 cm: reappraisal of the staging system for solitary tumors. *Ann. Surg. Oncol.* 2013; **20**; 1223–1229.

Research Article

EASL EUROPEAN ASSOCIATION FOR THE STUDY OF THE LIVER | JOURNAL OF HEPATOLOGY

Long-term native liver fibrosis in biliary atresia: Development of a novel scoring system using histology and standard liver tests

Hirofumi Tomita[1], Yohei Masugi[2], Ken Hoshino[1], Yasushi Fuchimoto[3], Akihiro Fujino[1], Naoki Shimojima[1], Hirotoshi Ebinuma[4], Hidetsugu Saito[4], Michiie Sakamoto[2], Tatsuo Kuroda[1,*]

[1]*Department of Pediatric Surgery, Keio University School of Medicine, 35 Shinanomachi, Shinjuku-ku, Tokyo 160-8582, Japan;* [2]*Department of Pathology, Keio University School of Medicine, 35 Shinanomachi, Shinjuku-ku, Tokyo 160-8582, Japan;* [3]*Division of Surgery, Department of Surgical Subspecialities, National Center for Child Health and Development, 2-10-1 Okura, Setagaya-ku, Tokyo 157-8535, Japan;* [4]*Department of Internal Medicine, Keio University School of Medicine, 35 Shinanomachi, Shinjuku-ku, Tokyo 160-8582, Japan*

Background & Aims: Although liver fibrosis is an important predictor of outcomes for biliary atresia (BA), postsurgical native liver histology has not been well reported. Here, we retrospectively evaluated postsurgical native liver histology, and developed and assessed a novel scoring system – the BA liver fibrosis (BALF) score for non-invasively predicting liver fibrosis grades.

Methods: We identified 259 native liver specimens from 91 BA patients. Of these, 180 specimens, obtained from 62 patients aged ⩾1 year at examination, were used to develop the BALF scoring system. The BALF score equation was determined according to the prediction of histological fibrosis grades by multivariate ordered logistic regression analysis. The diagnostic powers of the BALF score and several non-invasive markers were assessed by area under the receiver operating characteristic curve (AUROC) analyses.

Results: Natural logarithms of the serum total bilirubin, γ-glutamyltransferase, and albumin levels, and age were selected as significantly independent variables for the BALF score equation. The BALF score had a good diagnostic power (AUROCs = 0.86–0.94, p <0.001) and good diagnostic accuracy (79.4–93.3%) for each fibrosis grade. The BALF score revealed a strong correlation with fibrosis grade (r = 0.77, p <0.001), and was the preferable non-invasive marker for diagnosing fibrosis grades ⩾F2. In a serial liver histology subgroup analysis, 7/15 patients exhibited liver fibrosis improvement with BALF scores being equivalent to histological fibrosis grades of F0–1.

Conclusions: In postsurgical BA patients aged ⩾1 year, the BALF score is a potential non-invasive marker of native liver fibrosis.

Keywords: Biliary atresia; Hepatoportoenterostomy; Liver fibrosis; Liver biopsy; Non-invasive fibrosis marker.

Received 26 September 2013; received in revised form 18 December 2013; accepted 27 January 2014; available online 15 February 2014

* Corresponding author. Tel.: +81 3 5363 3024; fax: +81 3 3356 8804.

E-mail address: kuroda-t@z8.keio.jp (T. Kuroda).

Abbreviations: BA, biliary atresia; LT, liver transplantation; LDLT, living donor liver transplantation; BALF, biliary atresia liver fibrosis; PELD, pediatric end-stage liver disease; TB, total bilirubin; AST, aspartate aminotransferase; ALT, alanine aminotransferase; GGT, γ-glutamyltransferase; ChE, cholinesterase; PT-INR, prothrombin time-international normalized ratio; APRI, aspartate aminotransferase to platelet ratio index; PIIINP, procollagen type III amino-terminal peptide; AUROC, area under the receiver operating characteristic curve.

Introduction

Biliary atresia (BA) is a destructive, inflammatory, obliterative cholangiopathy that develops in 1/5,000 to 1/19,000 newborns [1]. The disease affects varying lengths of both the extra- and intra-hepatic bile ducts, and is classified according to the level of the most proximal part of the extra-hepatic biliary obstruction: atresia of the common bile duct (type 1), hepatic duct (type 2), or porta hepatis (type 3) [1,2]. To establish initial bile drainage, an anastomosis between the bile duct and the gastrointestinal tract can be created in certain cases ("correctable" BA, mostly type 1), but hepatoportoenterostomy is more often performed ("non-correctable" BA, mostly type 3) in such cases [2].

Hepatoportoenterostomy, first described by Kasai [3], can achieve initial bile drainage in 50–60% of cases [1]. However, liver fibrosis progresses rapidly before the bile drainage operation, and is an important predictor of outcome [4]. Even after successfully achieving bile drainage by portoenterostomy, progression of liver fibrosis may continue, leading to portal hypertension and cirrhosis [4]. Liver transplantation (LT) is performed when bile drainage is not achieved, or when complications of biliary cirrhosis occur [5]. Because of the progressive liver disease, long-term native liver survival is only achieved in approximately 20% of BA patients [4,5]. Thus, BA is the most common indication for LT in children; moreover, portoenterostomy is believed to be palliative, not curative [1].

Because of the severe shortage of organs from deceased donors in Japan [6], determination of the optimal time for living donor LT (LDLT) is important for BA patients. To investigate the postsurgical state of the native liver, we have performed percutaneous liver biopsies as part of the patient's routine follow-up. Because native liver fibrosis in postsurgical BA patients has not been well reported, we retrospectively analyzed the histology findings from 259 native liver specimens, and their associated

data, in 91 BA patients. From this, we developed a novel scoring system – the BA liver fibrosis (BALF) score – which is a non-invasive, practical, and easily accessible potential marker of liver fibrosis that is based on standard liver tests; its accuracy was also evaluated by comparing with the pediatric end-stage liver disease (PELD) score, which is widely used for liver allocation determinations [7], and the levels of several non-invasive fibrosis markers. Furthermore, we evaluated serial native liver histology in a subgroup of 15 patients.

Patients and methods

Study population and ethical considerations

We retrospectively identified 91 BA patients from whom native liver specimens had been obtained between March 1993 and February 2013 at Keio (Japan) University School of Medicine. The patients had either visited our institution for an initial operation, were referred to us for follow-up after an initial operation (42 patients), or had been referred to us due the presence of LT indicators (49 patients) after an initial operation for bile drainage. From the 91 patients, 259 liver specimens were collected by wedge biopsy during laparotomy (34 specimens), percutaneous needle biopsy (161 specimens), or were obtained from explanted livers during LT (64 specimens). From these specimens, we excluded 1 explanted liver because of a hepatitis C virus infection, and 18 specimens because of liver histology findings (described below).

Development of the BALF score was conducted from 180 histology examinations obtained from 62 patients aged ⩾1 year, because liver biochemistry results were likely elevated before surgery, and for a certain period after surgery, regardless of the liver fibrosis grade. Of the 180 specimens, the median number of specimens obtained from individual patients was 1 (range, 1–11). Of the 62 patients, 28 (45.2%) were male and 34 (54.8%) were female. Type 1 BA was diagnosed in 9 patients (14.5%), type 2 in 2 (3.2%), and type 3 in 45 (72.6%); the diagnosis was unknown in 6 (9.7%). The initial surgery for bile drainage was hepaticoenterostomy in 6 patients (9.7%), hepatoportoenterostomy in 54 (87.1%), and an unknown procedure in 2 (3.2%); the median age at the time of the initial surgery was 64 days (range, 17–151 days). Selection of the study population is summarized in Fig. 1. This study conformed to the ethical guidelines of the 1975 Declaration of Helsinki, and was approved by the ethical committee at Keio University School of Medicine (2012-173).

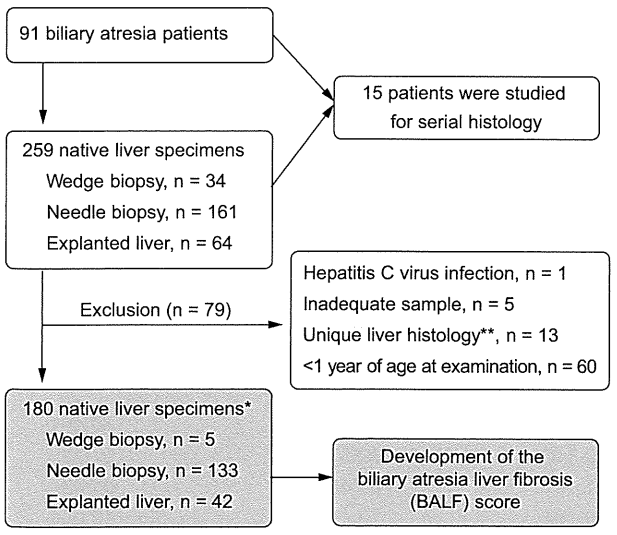

Fig. 1. Selection of the study population. *Obtained from 62 patients. **One patient revealed unique liver histology findings, indicating ductopenia, accompanied by little evidence of fibrosis in 13 serial percutaneous biopsies.

Data collection

The patients' clinical courses, documented pathological findings, and laboratory results around the time of liver specimen collection were collected from the patients' medical records. Collected standard biochemical test results included serum levels of total bilirubin (TB), aspartate aminotransferase (AST), alanine aminotransferase (ALT), γ-glutamyltransferase (GGT), albumin, and cholinesterase (ChE). Collected hematological test results included prothrombin time-international normalized ratios (PT-INR) and platelet counts. These standard biochemical and hematological test results were obtained for all corresponding histological examinations. The PELD score [7] was calculated using the following equation:

$$\text{PELD score} = \{0.463 \times (\text{age} < 1\,\text{year}^{*}) - 0.687 \times \text{Log}_{e}[\text{albumin (g/dl)}] + 0.480 \times \text{Log}_{e}[\text{TB (mg/dl)}] + 1.857 \times \text{Log}_{e}(\text{PT-INR}) + 0.667 \times (\text{growth failure} < -2\ \text{standard deviation}^{**})\} \times 10$$

*Age was coded as 1 for children under 1 year; in other cases, it was coded as 0.
**Growth failure was coded as 1 for children, with height or weight <−2 standard deviations below age-specific normal values; in other cases, it was coded as 0.

As a non-invasive fibrosis marker, the AST to platelet ratio index (APRI) [8] was also calculated; a serum AST level of 35 IU/L was used as the upper normal limit:

$$\text{APRI} = \{(\text{AST/upper normal limit})/[\text{platelet counts } (10^{9}/\text{L})]\} \times 100$$

The APRIs in patients having a history of splenectomy, partial splenic embolization, or with biliary atresia splenic malformation syndrome were excluded from further analyses. Direct serum fibrosis markers, including serum levels of hyaluronic acid, type IV collagen 7S domain, and procollagen type III amino-terminal peptide (PIIINP) [9], were collected for most of the corresponding histological examinations. The normal ranges are ⩽50.0 ng/ml for hyaluronic acid, ⩽6.0 ng/ml for type IV collagen 7S domain, and 0.30–0.80 U/ml for PIIINP.

Evaluation of liver histology

Wedge biopsy specimens, ⩾5 mm in size, were obtained by surgical resection from the edge of the liver during laparotomy. Percutaneous liver biopsies, ⩾1.0 cm in length, were performed with an 18-gauge suction needle under ultrasonographic guidance. All of the biopsies and operations were performed after obtaining written informed consent. The biopsy specimens and explanted livers were fixed in formalin, embedded in paraffin, sectioned, and stained with hematoxylin-eosin, Azan-Mallory, and Elastica van Gieson stains. Liver fibrosis was evaluated based on the documented pathological findings that had been reported at the time of examination by experienced pathologists, according to the METAVIR scoring system [10] or the new Inuyama classification [11] as follows: F0, no portal fibrosis; F1, portal fibrosis without septa; F2, portal fibrosis with rare septa; F3, numerous septa or lobular distortion without cirrhosis; and F4, cirrhosis. Five specimens, containing no or few portal tracts, were indeterminate for fibrosis grade. One patient revealed unique liver histology findings, indicating ductopenia, accompanied by little evidence of fibrosis in 13 serial percutaneous biopsies. When compared to the other subjects, the blood test results for this patient did not correspond to the histological fibrosis grade; therefore, these 13 specimens were excluded from the analysis.

Development of the BALF score by ordered logistic regression analysis

To predict the histological fibrosis grade, ordered logistic regression analyses were performed, using the histological fibrosis grades as ordinal data (F0, F1, F2, F3, and F4) for the dependent variable; the independent variables included logarithmic transformations of the collected standard biochemical and hematological test results, and age at the time of the corresponding histological examination. For multivariate logistic regression analysis, independent variables showing strong correlations (|r| >0.7) to each other were avoided because of multicollinearity concerns. The equation comprising the BALF score was developed by adding a minus sign to the regression equation for the logit of F0 probability in the multivariate analysis.

Table 1. Baseline data, stratified by histological fibrosis grade, for the development of the biliary atresia liver fibrosis (BALF) score.

	F0 (n = 15)	F1 (n = 53)	F2 (n = 44)	F3 (n = 34)	F4 (n = 34)
TB (mg/dl)	0.5 (0.2-0.9)	0.7 (0.3-10.1)	0.8 (0.3-11.5)	1.9 (0.4-24.5)	7.2 (0.3-30.1)
AST (IU/L)	33 (25-83)	36 (18-550)	75 (22-251)	108 (35-1065)	181 (94-472)
ALT (IU/L)	22 (14-79)	35 (9-676)	64 (13-457)	86 (21-411)	133 (37-587)
GGT (IU/L)	44 (10-102)	68 (7-1108)	142 (8-1384)	204 (66-1456)	317 (32-1817)
Albumin (g/dl)	4.4 (3.7-4.7)	4.1 (3.1-5.1)	4.0 (3.0-5.1)	3.7 (2.4-4.6)	3.2 (1.5-4.5)
ChE (IU/L)	326 (220-598)	342 (97-567)	278 (122-581)	185 (46-335)	141 (43-323)
PT-INR	1.07 (1.00-1.21)	1.07 (0.91-1.47)	1.03 (0.86-1.25)	1.04 (0.86-2.01)	1.14 (0.89-1.48)
Platelet count (× 10^9/L)	141 (70-356)	165 (52-372)	127 (45-392)	113 (56-446)	152 (42-524)
Age (yr)	9.7 (1.1-18.8)	7.0 (1.2-19.9)	5.3 (1.2-19.2)	7.4 (1.1-25.4)	2.4 (1.0-33.6)

Data are presented as median (range).
TB, total bilirubin; AST, aspartate aminotransferase; ALT, alanine aminotransferase; GGT, γ-glutamyltransferase; ChE, cholinesterase; PT-INR, prothrombin time-international normalized ratio.

Assessment of the BALF score

After developing the BALF score equation, the score at the time of each histological examination was calculated. The BALF score and other non-invasive markers were assessed in the same population that was used for development of the BALF score equation. We also calculated and evaluated the BALF score results in patients aged <1 year before and after bile drainage surgery.

Analysis of serial liver histology and the BALF score in each patient

Among the 91 patients involved in this study, 31 underwent histological examinations at the time of their initial operation during the study period. Of these, 15 had repeated histological examinations when they were aged ⩾2 years and these patients were individually analyzed to obtain serial data. Among the other 16 patients, 4 underwent primary LDLT; 1 died suddenly at 11 months of age; 5 underwent LDLT before 2 years of age; 5 were <2 years of age at the time of this analysis; and 1 patient, who had undergone hepaticoenterostomy for type 2 BA, did not undergo a histological examination after reaching 2 years of age.

Statistical analysis

The categorical data are presented as frequencies (%), and the continuous data are presented as medians (ranges). Correlations between the ordinal and/or continuous data were assessed by Spearman's correlation coefficient (r). For logistic regression analyses, the *p* value of each independent variable was determined by the Wald chi-square value (Wald), which was calculated by squaring the ratio of the regression coefficient divided by its standard error. The diagnostic powers of the BALF score and the other fibrosis markers were assessed by area under the receiver operating characteristic curve (AUROC) analyses; an AUROC of 1.0 indicates a test of perfect diagnostic power, and that of 0.5 indicates a test without diagnostic power. The cut-off values were determined by maximizing the sum of the sensitivity and specificity on Youden's index [12]. *p* values <0.05 were considered statistically significant. Statistical analyses were performed using SPSS 20.0 software (IBM SPSS, Chicago, IL, USA).

Results

Development of the BALF score by ordered logistic regression analysis

Baseline data corresponding to the 180 histology examinations for the development of the BALF score, stratified by histological fibrosis grade, are summarized in Table 1; the results of the ordered logistic regression analyses are shown in Table 2. In the univariate analyses, natural logarithms of the serum TB levels provided the most significant coefficients (Wald = 89.240, p <0.001). In the multivariate analysis, natural logarithms of the

Table 2. Ordered logistic regression analyses for liver fibrosis grades, F0–F4.

Variable	Coefficient (95% CI)	Standard error	Wald	*p* value
Univariate analysis				
Log_e [TB (mg/dl)]	1.854 (1.470-2.239)	0.196	89.240	<0.001
Log_e [AST (IU/L)]	1.926 (1.493-2.358)	0.221	76.107	<0.001
Log_e [ALT (IU/L)]	1.218 (0.886-1.550)	0.169	51.737	<0.001
Log_e [GGT (IU/L)]	0.858 (0.617-1.100)	0.123	48.448	<0.001
Log_e [albumin (g/dl)]	-8.017 (-10.139--5.896)	1.082	54.871	<0.001
Log_e [ChE (IU/L)]	-3.218 (-3.948--2.487)	0.373	74.527	<0.001
Log_e [PT-INR]	2.627 (0.342-4.913)	1.166	5.078	0.02
Log_e [platelet count (× 10^9/L)]	-0.299 (-0.799-0.202)	0.255	1.370	0.24
Log_e [age (years)]	-0.438 (-0.742--0.134)	0.155	7.994	0.005
Multivariate analysis				
Log_e [TB (mg/dl)]	1.438 (0.974-1.903)	0.237	36.861	<0.001
Log_e [GGT (IU/L)]	0.434 (0.159-0.710)	0.140	9.557	0.002
Log_e [albumin (g/dl)]	-3.491 (-5.805--1.177)	1.181	8.745	0.003
Log_e [age (years)]	-0.670 (-1.031--0.308)	0.184	13.196	<0.001

TB, total bilirubin; AST, aspartate aminotransferase; ALT, alanine aminotransferase; GGT, γ-glutamyltransferase; ChE, cholinesterase; PT-INR, prothrombin time-international normalized ratio.

Table 3. Diagnostic accuracy of the biliary atresia liver fibrosis (BALF) score in predicting histological fibrosis grade.

	AUROC	95% CI	Cut-off	Sensitivity	Specificity	Accuracy
≥F1	0.91*	0.86-0.96	1.96	77.6%	100%	79.4%
≥F2	0.86*	0.81-0.92	2.42	86.6%	73.5%	81.7%
≥F3	0.91*	0.87-0.95	4.12	83.8%	81.3%	82.2%
=F4	0.94*	0.90-0.99	5.64	94.1%	93.2%	93.3%

*p <0.001.
AUROC, area under the receiver operating characteristic curve.

serum TB, GGT, and albumin levels, and age at examination were selected as significant independent variables. Based on the multivariate analysis, the BALF score equation was developed:

$$\text{BALF score} = 7.196 + 1.438 \times \text{Log}_e[\text{TB (mg/dl)}] + 0.434 \times \text{Log}_e[\text{GGT (IU/L)}] - 3.491 \times \text{Log}_e[\text{albumin (g/dl)}] - 0.670 \times \text{Log}_e[\text{age (years)}]$$

Diagnostic accuracy of the BALF score

Table 3 shows the AUROC, cut-off value, and diagnostic accuracy of the BALF score for each fibrosis grade. The BALF score had good diagnostic power for predicting each fibrosis grade (AUROCs = 0.86–0.94, p <0.001), and the cut-off values were calculated as 1.96 for a fibrosis grade ⩾F1, 2.42 for ⩾F2, 4.12 for ⩾F3, and 5.64 for F4; the score provided good diagnostic accuracy in diagnosing each fibrosis grade (79.4–93.3%).

Comparisons of the BALF score, PELD score, and other non-invasive fibrosis markers

Fig. 2 shows the boxplots for the BALF score, PELD score, APRI, and levels of serum hyaluronic acid, type IV collagen 7S domain, and PIIINP *vs.* the histological fibrosis grade. Of these, the BALF score was most strongly correlated with the histological fibrosis grade (r = 0.77, p <0.001). The BALF score was equally distributed from F0 to F4. The diagnostic powers of the BALF score and the other markers for diagnosing fibrosis grades ⩾F2 and F4, assessed by AUROC analyses, are shown in Fig. 3. For diagnosing fibrosis grades ⩾F2, the BALF score had the highest diagnostic power (AUROC = 0.86, p <0.001), followed by the PELD score and the APRI (AUROC = 0.80, p <0.001), but the direct serum markers showed relatively low or no significant diagnostic power. The PELD score, hyaluronic acid levels, and type IV collagen 7S domain levels, as well as the BALF score, showed excellent diagnostic powers for diagnosing an F4 fibrosis grade (AUROC >0.90, p <0.001).

Changes in the BALF score before and after bile drainage surgery

The BALF scores for patients aged <1 year, before and after initial surgery (n = 31 and n = 29, respectively), compared to patients aged 1–2 years, after surgery (n = 28), are shown in Fig. 4. The BALF scores were apparently high before surgery, regardless of the fibrosis grades. Even after bile drainage surgery, patients aged <1 year showed high score values. The BALF scores in the patients aged 1–2 years were comparable with those for all patients aged ⩾1 year.

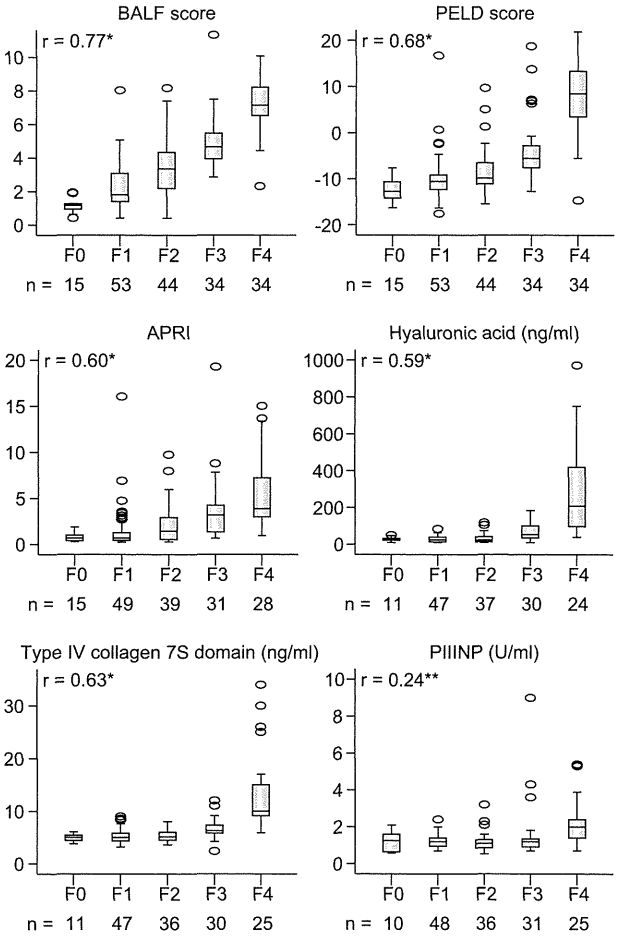

Fig. 2. Comparisons of the biliary atresia liver fibrosis (BALF) score, the pediatric end-stage liver disease (PELD) score, and several non-invasive fibrosis markers. Boxplots show the median values with the interquartile ranges, and error bars indicate the smallest and the largest values within 1.5 box-lengths of the upper and the lower quartiles. Outliers represent the individual points by circles. Correlations between the scores/markers and the histological fibrosis grades were evaluated by Spearman's correlation coefficient (r); *p <0.001, **p = 0.009. APRI, aspartate aminotransferase to platelet ratio index; PIIINP, procollagen type III amino-terminal peptide.

Serial liver histology and BALF score in each patient

The status of the initial operations and the most recent histological examinations for 15 patients are shown in Table 4. Cases 1–7 showed some liver fibrosis relief with BALF scores being equivalent to F0–1; these 7 patients achieved good physical growth and

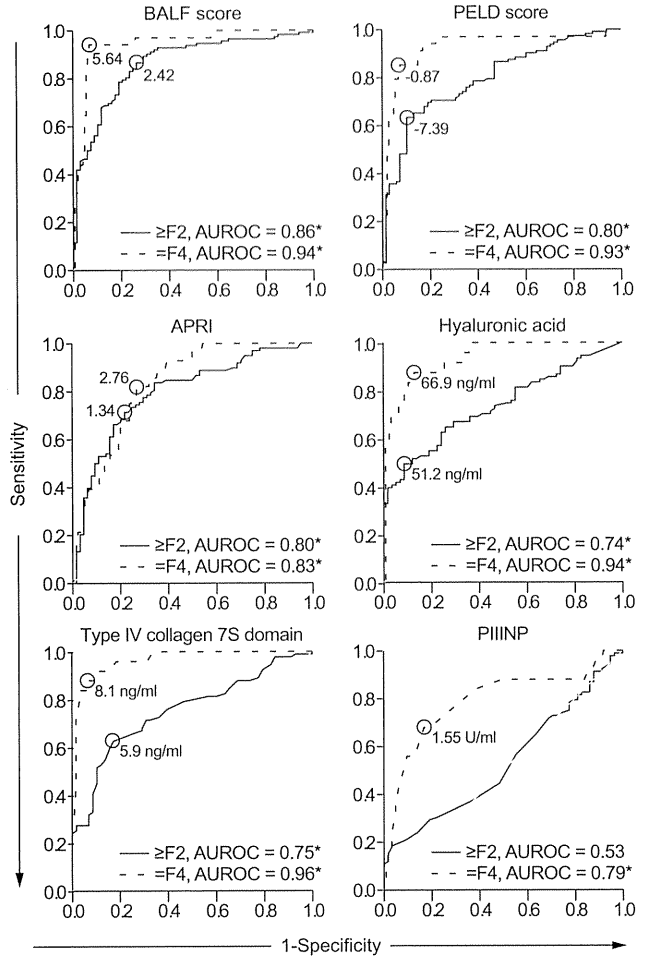

Fig. 3. The diagnostic powers of the biliary atresia liver fibrosis (BALF) score, pediatric end-stage liver disease (PELD) score, and non-invasive markers for liver fibrosis. The diagnostic power of each score/marker was assessed by calculating the area under the receiver operating characteristic curve (AUROC); solid lines, for diagnosing ⩾F2; dashed lines, for diagnosing F4; gray lines, reference lines; circles, cut-off points (with cut-off values); *p <0.001. APRI, aspartate aminotransferase to platelet ratio index; PIIINP, procollagen type III amino-terminal peptide.

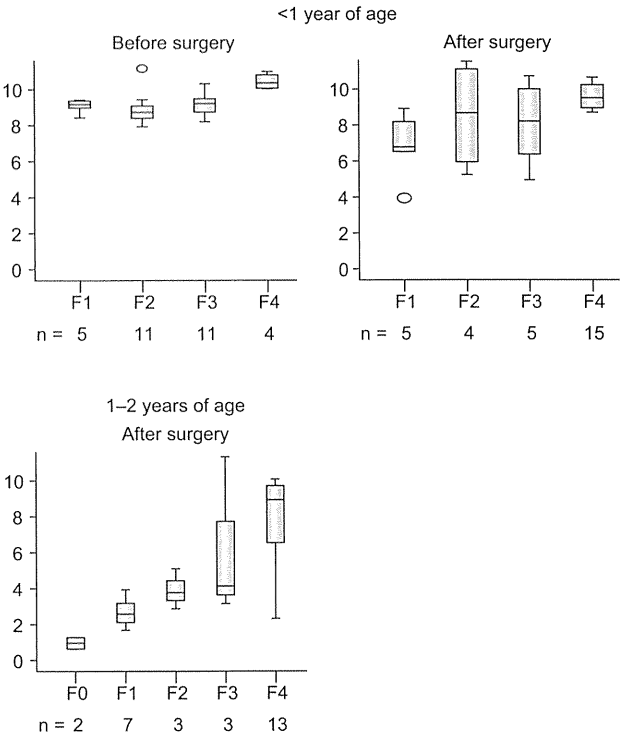

Fig. 4. Changes in the BALF score, before and after bile drainage surgery. Boxplots show the median values with the interquartile ranges, and error bars indicate the smallest and the largest values within 1.5 box-lengths of the upper and the lower quartiles. Outliers represent the individual points by circles.

social activity. Cases 8–12 showed the same grade of fibrosis in the initial and latest histological examinations; 3 of them had shown initial transient relief of liver fibrosis followed by worsening fibrosis, associated with repetitive cholangitis (Cases 10 and 11) or hepatopulmonary syndrome (Case 12). Cases 13–15 showed worsening liver fibrosis and relatively high BALF scores. Only Case 12 underwent LT during the study period; Cases 13–15 seemed likely to require LT in the near future due the presence of severe portal hypertension.

Discussion

Although hepatoportoenterostomy can achieve complete jaundice resolution in up to 60% of children with BA, liver fibrosis – a prominent feature of BA – may continue to progress [1,4,5]. Although LT in children with failed bile drainage surgery is certain, the timing of LT after successful bile drainage is debatable [13]. In Japan, grafts for LT rely almost entirely on living donors, especially from the parents of affected children [6]. Due to the increasing parental age and the required graft volume against the physical growth of the recipients, LDLT may not be possible, in some cases. Moreover, one large Japanese study indicated poor outcomes of adult-to-adult LDLT for postoperative BA patients, and the authors encouraged proactive consideration of LDLT at the earliest possible stage [14]. At our institution, hepatoportoenterostomy and LT for BA patients have been performed by the same team since the introduction of LDLT in 1995. To assess the native liver status more precisely, we introduced liver biopsies as the gold standard method for assessing liver fibrosis, with endoscopic screening of postsurgical BA patients. At first, liver fibrosis was supposed to progress in most BA patients, suggesting the future need for LT; only stable disease was believed to provide the patients and their parents with some relief. Thereafter, we noticed that certain patients demonstrated fibrosis improvement. Concerns about biopsy sampling errors were alleviated by serial liver histology, thus providing more substantial relief.

The BALF regression equation suggests that long-term native liver fibrosis in BA is influenced by the patient's bile drainage status, represented by the levels of serum TB and GGT. Some patients, especially older children or adults, develop decreasing liver synthetic capacity despite relatively small elevations in serum TB levels (data not shown). Thus, serum albumin levels represent a significant negative coefficient in the multivariate ordered logistic regression analysis. Additionally, the age at examination also showed a significant negative coefficient, suggesting that liver fibrosis could be improved over time, even in

Table 4. The status of 15 patients individually examined by serial liver histology.

Case No.	Disease type	Initial operation			Recent histological examination		
		Age (days)	Procedure	Fibrosis grade	Age (years)	Fibrosis grade	BALF score
1	Type 1	17	Hepaticoenterostomy	F2	2.5	F0	1.26
2	Type 1	24	Hepaticoenterostomy	F3	12.5	F1	1.17
3	Type 1	31	Portoenterostomy	F2	6.4	F1	1.50
4	Type 1	55	Portoenterostomy	F2	11.0	F0	1.26
5	Type 3	78	Portoenterostomy	F3	3.3	F1	2.12
6	Type 3	74	Portoenterostomy	F3	18.3	F1	0.84
7	Type 3	74	Portoenterostomy	F2	18.8	F0	1.19
8	Type 3	47	Portoenterostomy	F2	7.1	F2	2.44
9	Type 3	47	Portoenterostomy	F1	14.8	F1	2.34
10	Type 3	105	Portoenterostomy	F2	7.8	F2	2.20
11	Type 3	51	Portoenterostomy	F3	8.1	F3	3.24
12	Type 3	105	Portoenterostomy	F3	9.3	F3	4.84
13	Type 3	56	Portoenterostomy	F1	9.3	F2	3.94
14	Type 3	56	Portoenterostomy	F1	7.1	F3	4.68
15	Type 3	57	Portoenterostomy	F2	3.5	F3	6.26

BALF, biliary atresia liver fibrosis.

BA patients. Recently, liver fibrosis has been indicated to be reversible in a number of liver diseases, but data for BA are limited [4]. A few serial liver histology reports from the 1960s to 1980s documented fibrosis relief in some cases [15–18]. Thereafter, only a few studies have involved postsurgical liver histology [19,20]; however, serial data have not been presented. In a subpopulation of the current study, 7 of the 15 patients who achieved long-term native liver survival revealed some liver fibrosis relief during the study period.

The BALF score is the first non-invasive fibrosis marker developed for postsurgical BA patients based on liver histology findings, including the findings of percutaneous needle biopsy examinations obtained from patients with good postoperative courses. However, the PELD score was developed based on poor outcomes, such as patient death or movement to an intensive care unit, in children awaiting LT [7,21]. Although the BALF and PELD scores share the same independent variables (natural logarithms of serum TB and albumin levels), the BALF score results were more spread out than the PELD score results in the low fibrosis grade groups (F0–F3); moreover, the PELD score results were more spread out among the patients with cirrhosis (F4) than were the BALF score results (Fig. 1). Thus, the BALF score appears to be suitable for all patients (F0–4), but the PELD score seems best suited for severely affected patients, such as those with cirrhosis (F4), reflecting the methods used for the development of each score. The APRI consists of only two variables, is much simpler to calculate, and has been investigated in relation to prognosis [22], portal venous pressure [23], and fibrosis grade [24] at the time of Kasai hepatoportoenterostomy. Moreover, the APRI was used as a surrogate fibrosis marker in a prospective study examining steroid therapy in BA patients [25].

Although the current study contains one of the largest series of native liver histologies reported for BA patients, several limitations remain. First, the current study used liver histology findings, obtained from liver biopsies or explanted liver examinations, as reference parameters. Since biopsies are limited by sampling errors [26] and observer variability [27], the histological results are subject to omissions and false-positive results. In addition, segmental bile drainage, often observed in postsurgical BA patients [28] or small biopsy samples, may have resulted in an increased level of sampling error [26]. Second, this study had a relatively small sample size and a heterogeneous study population. Not all of the patients were evaluated by serial liver histology, after surgery, and the number of examinations in the same patient also differed; we analyzed the data from the same patient as independent data. We could not provide a validation group for the newly developed BALF scoring system because of the small and heterogeneous study population.

In the present study, we developed a potential fibrosis marker for postsurgical BA patients that is non-invasive, practical, and easily accessible. Because of a lack of validation, the BALF score should be further investigated with regard to its relationship with several parameters, such as long-term outcomes, postsurgical complications, and liver fibrosis. However, we believe that the BALF score will be a useful surrogate fibrosis marker in a future interventional trial.

Financial support

This study was supported by a grant from The Ministry of Health, Labour and Welfare of Japan (H24-Nanchi-Ippan-037, Health Labour Sciences Research Grants for Research on intractable diseases).

Conflict of interest

The authors who have taken part in this study declared that they do not have anything to disclose regarding funding or conflict of interest with respect to this manuscript.

References

[1] Hartley JL, Davenport M, Kelly DA. Biliary atresia. Lancet 2009;374:1704–1713.

[2] Nio M, Ohi R. Biliary atresia. Semin Pediatr Surg 2000;9:177–186.

[3] Kasai M, Suzuki S. A new operation for "noncorrectable" biliary atresia; hepatic portoenterostomy. Shujutsu (Operation) 1959;13:733–739. [In Japanese].
[4] Haafiz AB. Liver fibrosis in biliary atresia. Expert Rev Gastroenterol Hepatol 2010;4:335–343.
[5] Lykavieris P, Chardot C, Sokhn M, Gauthier F, Valayer J, Bernard O. Outcome in adulthood of biliary atresia: a study of 63 patients who survived for over 20 years with their native liver. Hepatology 2005;41:366–371.
[6] Tanabe M, Kawachi S, Obara H, Shinoda M, Hibi T, Kitagawa Y, et al. Current progress in ABO-incompatible liver transplantation. Eur J Clin Invest 2010;40:943–949.
[7] Freeman Jr RB, Wiesner RH, Harper A, McDiarmid SV, Lake J, Edwards E, et al. The new liver allocation system: moving toward evidence-based transplantation policy. Liver Transpl 2002;8:851–858.
[8] Wai CT, Greenson JK, Fontana RJ, Kalbfleisch JD, Marrero JA, Conjeevaram HS, et al. A simple non-invasive index can predict both significant fibrosis and cirrhosis in patients with chronic hepatitis C. Hepatology 2003;38:518–526.
[9] Gressner OA, Weiskirchen R, Gressner AM. Biomarkers of liver fibrosis: clinical translation of molecular pathogenesis or based on liver-dependent malfunction tests. Clin Chim Acta 2007;381:107–113.
[10] Bedossa P, Poynard T. An algorithm for the grading of activity in chronic hepatitis C. The METAVIR Cooperative Study Group. Hepatology 1996;24:289–293.
[11] Ichida F, Tsuji T, Omata M, Ichida T, Inoue K, Kamimura T, et al. New Inuyama classification; new criteria for histological assessment of chronic hepatitis. Int Hepatol Commun 1996;6:112–119.
[12] Youden WJ. Index for rating diagnostic tests. Cancer 1950;3:32–35.
[13] Kyoden Y, Tamura S, Sugawara Y, Yamashiki N, Matsui Y, Togashi J, et al. Outcome of living donor liver transplantation for post-Kasai biliary atresia in adults. Liver Transpl 2008;14:186–192.
[14] Uchida Y, Kasahara M, Egawa H, Takada Y, Ogawa K, Ogura Y, et al. Long-term outcome of adult-to-adult living donor liver transplantation for post-Kasai biliary atresia. Am J Transplant 2006;6:2443–2448.
[15] Bunton GL, Cameron R. Regeneration of liver after biliary cirrhosis. Ann N Y Acad Sci 1963;111:412–421.
[16] Altman RP, Chandra R, Lilly JR. Ongoing cirrhosis after successful portico-enterostomy in infants with biliary atresia. J Pediatr Surg 1975;10:685–691.
[17] Kasai M, Watanabe I, Ohi R. Follow-up studies of long term survivors after hepatic portoenterostomy for "noncorrectable" biliary atresia. J Pediatr Surg 1975;10:173–182.
[18] Gautier M, Valayer J, Odievre M, Alagille D. Histological liver evaluation 5 years after surgery for extrahepatic biliary atresia: a study of 20 cases. J Pediatr Surg 1984;19:263–268.
[19] Hasegawa T, Sasaki T, Kimura T, Hoki M, Okada A, Mushiake S, et al. Measurement of serum hyaluronic acid as a sensitive marker of liver fibrosis in biliary atresia. J Pediatr Surg 2000;35:1643–1646.
[20] Hadzic N, Davenport M, Tizzard S, Singer J, Howard ER, Mieli-Vergani G. Long-term survival following Kasai portoenterostomy: is chronic liver disease inevitable? J Pediatr Gastroenterol Nutr 2003;37:430–433.
[21] McDiarmid SV, Anand R, Lindblad AS. Principal Investigators and Institutions of the Studies of Pediatric Liver Transplantation Research Group. Development of a pediatric end-stage liver disease score to predict poor outcome in children awaiting liver transplantation. Transplantation 2002;74:173–181.
[22] Grieve A, Makin E, Davenport M. Aspartate Aminotransferase-to-Platelet ratio index (APRi) in infants with biliary atresia: prognostic value at presentation. J Pediatr Surg 2013;48:789–795.
[23] Shalaby A, Makin E, Davenport M. Portal venous pressure in biliary atresia. J Pediatr Surg 2012;47:363–366.
[24] Kim SY, Seok JY, Han SJ, Koh H. Assessment of liver fibrosis and cirrhosis by aspartate aminotransferase-to-platelet ratio index in children with biliary atresia. J Pediatr Gastroenterol Nutr 2010;51:198–202.
[25] Davenport M, Parsons C, Tizzard S, Hadzic N. Steroids in biliary atresia: Single surgeon, single centre, prospective study. J Hepatol 2013;59:1054–1058.
[26] Bedossa P, Dargere D, Paradis V. Sampling variability of liver fibrosis in chronic hepatitis C. Hepatology 2003;38:1449–1457.
[27] Bedossa P. The French METAVIR Cooperative Study Group. Intraobserver and interobserver variations in liver biopsy interpretation in patients with chronic hepatitis C. Hepatology 1994;20:15–20.
[28] Takahashi A, Masuda N, Suzuki M, Shimura T, Nomoto K, Suzuki N, et al. Evidence for segmental bile drainage by hepatic portoenterostomy for biliary atresia: cholangiographic, hepatic venographic, and histologic evaluation of the liver taken at liver transplantation. J Pediatr Surg 2004;39:1–5.

Proc. of 2014 IEEE International Ultrasonics Symposium, 2014.

Shear wave elasticity imaging using inverse filtering and multiple-point shear wave generation

Tomoaki Kitazaki, Tsuyoshi Shiina
Graduate School of Medicine
Kyoto University
Kyoto, Japan
kitazaki@shiina-lab.hs.med.kyoto-u.ac.jp

Kengo Kondo, Makoto Yamakawa
Center for the Promotion of Interdisciplinary Education and Research
Kyoto University
Kyoto, Japan

Abstract— **Estimating shear wave speed enables quantifying tissue elasticity imaging using time-of-flight, but measurement of time-of-flight is based on an assumption about the propagating direction of a shear wave that is highly affected by reflection and refraction and thus might cause an artifact. An alternative shear elasticity estimation approach based on shear wavelength was proposed and applied to passive configurations. We propose a new method for shear wave elasticity imaging that combines the shear wavelength approach and "active" acoustic pushing configuration, i.e., the multiple shear wave sources induced by acoustic radiation force (ARF). The feasibility of the proposed method was verified using an elasticity phantom with a hard inclusion.**

Keywords—tissue elasticity imaging, shear wave, inverse filter, acoustic radiation force

I. Introduction

Tissue elasticity is measured in the diagnosis of tissue diseases such as cancer and liver fibrosis since it is related to the pathological condition. For example, in a mammary grand, higher grade malignancies yield harder tumors [1]. Shear wave speed is directly linked to the tissue elasticity. Radiation from a focused ultrasound beam has been used to produce shear waves, and the time-of-flight is measured to determine the shear wave speed [2]. However, the method is based on an assumed propagating direction of a shear wave that is highly affected by reflection and refraction and thus might cause an artifact.

An alternative shear elasticity estimation approach based on shear wavelength [3] was proposed and applied to passive configurations. This method is not based on an assumed propagating direction and so is expected to improve the estimation accuracy. However, it requires longer acquisition time than the conventional method.

To acquire elasticity of tissue faster and more accurately, we propose a new method for shear wave elasticity imaging that combines the shear wavelength approach and an "active" acoustic pushing configuration, i.e., the multiple shear wave sources induced by acoustic radiation force (ARF). An inverse filter can be achieved more efficiently using ARF sources than using passive configurations because the shear wave generation can be controlled and the shear waves induced by the acoustic radiation force impulses are good approximations of the impulse responses of shear wave excitation. An inverse filter can focus a point in a reverberant field. Thus, the proposed method is not based on the assumption of the propagating direction, and improved estimation accuracy can be expected. This study demonstrates the feasibility of the proposed method with phantom experiments.

II. Metohods of Elasticity Imaging

A. Overall Flow

Shear waves generated at widely separated pushing points are recorded by an ultrafast imaging method. Assuming that ARFs are impulses at each push point, shear waves measured at an arbitrary point are approximated as impulse responses. An inverse filter [4] can be applied to virtually focus a shear wave on an arbitrary point. Measuring the full width at half maximum (FWHM) of the focal point is equivalent to the half-wavelength of the shear wave, and the shear-elasticity is obtained through the shear wave speed. A shear-elasticity image can be obtained by scanning the focal point.

B. Inverse Filter

In the Fourier domain, receiving column vector $\mathbf{R}(\omega)$ is referred to in the product of the propagation matrix $\mathbf{H}(\omega)$ and the emission column vector $\mathbf{E}(\omega)$.

$$\mathbf{R}(\omega) = \mathbf{H}(\omega) \cdot \mathbf{E}(\omega), \tag{1}$$

Here, ω is the given frequency. $\mathbf{H}(\omega)$ has all the information of the propagation effects in the medium.

The inverse filter approach consists of choosing an objective vector $\mathbf{R}_j^{IF}(\omega)$ for the receiving vector. Only point j of $\mathbf{R}_j^{IF}(\omega)$ is 1, the others are 0. $\mathbf{R}_j^{IF}(\omega)$ is given by

$$\mathbf{R}_j^{IF}(\omega) = \mathbf{H}(\omega) \cdot \mathbf{E}_j^{IF}(\omega). \tag{2}$$

$\mathbf{R}_j^{IF}(\omega)$ and $\mathbf{H}(\omega)$ are given. To find $\mathbf{E}_j^{IF}(\omega)$, multiply the inverse matrix $\mathbf{H}^{-1}(\omega)$ from the left of $\mathbf{H}(\omega)$. However, this process magnifies errors. Thus, before inversion, a singular value decomposition of $\mathbf{H}(\omega)$ is performed. The matrix

inversion is only applied to the main singular vectors of the singular value decomposition of $\mathbf{H}(\omega)$. This can prevent the inversion of noise components. The ideal emission $\tilde{\mathbf{E}}_j^{IF}(\omega)$ is then derived by

$$\begin{aligned}\tilde{\mathbf{H}}^{-1}(\omega)\cdot\mathbf{R}_j^{IF}(\omega) &= \tilde{\mathbf{H}}^{-1}(\omega)\cdot\mathbf{H}(\omega)\cdot\mathbf{E}_j^{IF}(\omega) \\ &= \tilde{\mathbf{E}}_j^{IF}(\omega),\end{aligned} \tag{3}$$

where $\tilde{\mathbf{H}}^{-1}(\omega)$ is the noise-filtered inverse matrix.

The optimal focusing $\psi_j(\omega)$ will be derived by

$$\psi_j(\omega) = \mathbf{H}(\omega)\cdot\tilde{\mathbf{H}}^{-1}(\omega)\cdot\mathbf{R}_j^{IF}(\omega). \tag{4}$$

An inverse filter was then applied to focus shear waves on a central point in a simulation (Fig. 1(a)).

C. *Method of Measuring Young's modulus*

Young's modulus is the three times of the square of shear speed. The shear wave speed can be measured by calculating the product of the shear wavelength and the frequency. The half-wavelength of the shear wave can be obtained by measuring the FWHM of the focal point (Fig. 1(b)) [5].

III. Exprtimental Condision

An elasticity phantom with 10 mm diameter hard inclusions (OST, Japan) was prepared. The characteristics given by the manufacturer are 40, 60, 80, and 100 kPa for the inclusions and 10 kPa for the background (BG). Fig. 2(a) presents a schematic view of the experiment conditions. This study used inclusions of 60 and 80 kPa. The pushing domain (axial 37.5mm, lateral 38.4mm) is marked with broken lines. Fig. 2(b) depicts pushing points. The B-modes of 60 kPa (Fig. 2(c)) and 80 kPa (Fig. 2(d)) indicate the border of hard inclusions and BG.

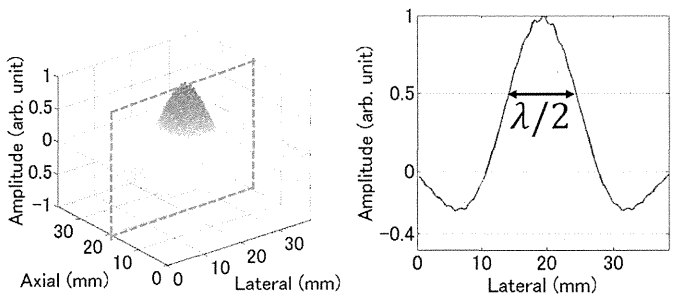

(a) (b)

Fig. 1 (a) 2D map and (b) lateral profile of focused shear wave in a simulation.

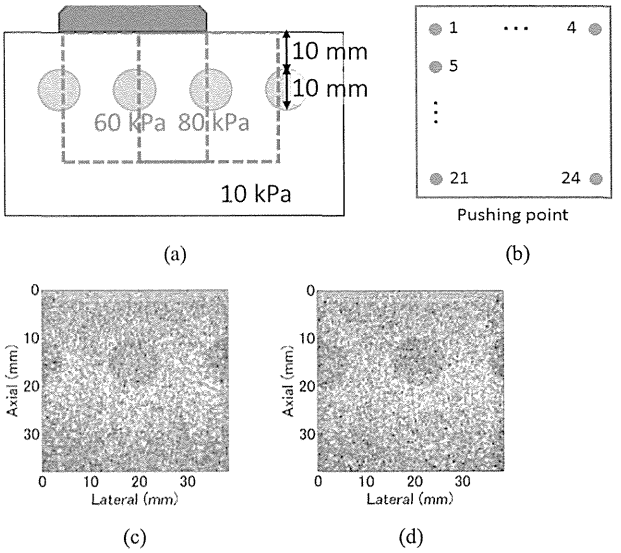

(a) (b)

(c) (d)

Fig. 2 (a) Schematic view of experimental condition. (b) Pushing points. B-mode of the elasticity phantom with (c) 60 kPa inclusion (d) 80 kPa inclusion.

A Verasonics ultrasound system with a 128-channel linear-array transducer was used to implement the proposed method. The center frequency is 5 MHz, and the frame rate is 5 kHz. Multiple (24) pushing points were sparsely generated with intervals of 6 mm (axial) and 9 mm (lateral). ARF was applied for 78 μs, and 32 times averaging was performed. The ultrasonic diagnosis recording time was 24 ms per push point. Frequencies of 200–300 Hz were used for making elasticity maps.

IV. Elasticity Imaging

The proposed method was validated by phantom experiments. To compare the conventional method, Aixplorer (Supersonicimagine Inc.) was used. Fig. 3(a) shows the estimated elasticity image of nearby the hard inclusion obtained from the proposed method. Fig. 3(b) shows the profile along the dotted line in Fig. 3(a). Fig. 4(a) shows the estimated elasticity image of nearby the hard inclusion obtained from the conventional method. Fig. 4(b) shows the profile along the dotted line in Fig. 4(a). Fig. 5(a) and 6(a) show several elastic maps, and Fig. 5(b) and 6(b) show several lateral profile (inclusion 80 kPa), we could get results that is same as results of 60 kPa.

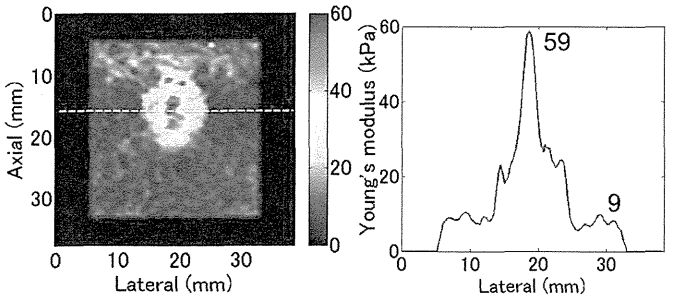

(a) (b)

Fig. 3 (a) Estimated elasticity image and (b) lateral profile of the proposed method (60 kPa inclusion).

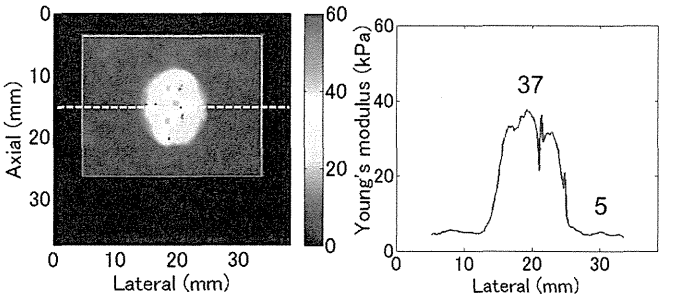

(a) (b)

Fig. 4 (a) Estimated elasticity image and (b) lateral profile of the time-of-flight-based method (60 kPa inclusion).

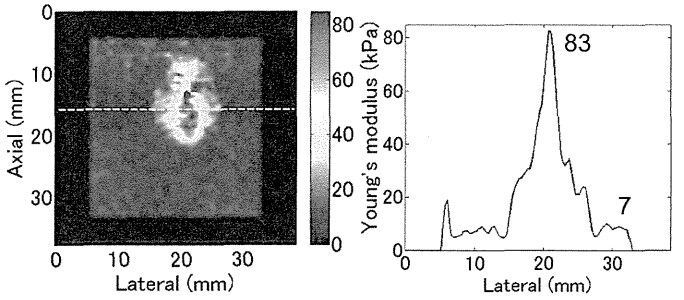

(a) (b)

Fig. 5 (a) Estimated elasticity image and (b) lateral profile of the proposed method (80 kPa inclusion).

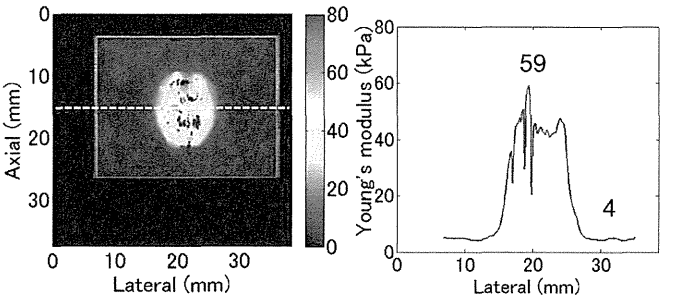

(a) (b)

Fig. 6 (a) Estimated elasticity image and (b) lateral profile of the time-of-flight-based method (inclusion: 80 kPa).

Both the proposed and the conventional methods could visualize the inclusion. The estimated value from the proposed method and the given value agreed well. The elasticity had a peak in the profile of the proposed method. Around the border, the FWHM exceeded the inclusion diameter, possibly causing an error. The feasibility of the proposed method was verified, but we have to seek an alternative approach to measure the shear wavelength.

V. Conclusions

We proposed a new method for estimating tissue elasticity that combines the shear wavelength approach and multiple shear wave sources induced by ARF. The feasibility of the proposed method was verified using a phantom with an inclusion having different elasticity than the background. The estimated elasticity image clearly revealed the hard inclusion.

The influence of reflection and refraction must be confirmed by the comparison between the proposed and conventional methods in greater detail.

References

[1] A. Samani1, J. Zubovits, and D. Plewes, "Elastic moduli of normal and pathological human breast tissues: an inversion-technique-based investigation of 169 samples," Phys. Med. Biol. vol. 52, pp. 1565–1576, March 2007.

[2] M. Tanter et al., "Quantitative assessment of breast lesion viscoelasticity: initial clinical resuluts using supersonic shear imaging," Ultrasound in Med. & Biol., vol. 34, pp. 1373–1386, September 2008.

[3] T. Gallot, S. Catheline, P. Roux, and M. Campillo "A passive inverse filter for Green's function retrieval," J. Acoust. Soc. Am., vol. 131, pp. EL21–27, January 2012.

[4] M. Tanter, J. F. Aubry, J. Gerber, J. L. Thomas, and M. Fink, "Optimal focusing by spatio-temporal inverse filter. I. Basic principles," J. Acoust. Soc. Am., vol. 110, pp. 37–47, July 2001.

[5] N. Benech, S. Catheline, J. Brum, T. Gallot, and C. A. Negreria: "1-D Elasticity Assessment in Soft Solid from Shear Wave Correlation: The Time-Reversal Approach," IEEE Trans. Ultrason. Ferroelctr. Freq. Control, vol. 56, pp. 2400-2410, November 2009.

Curr Pathobiol Rep (2014) 2:209–215
DOI 10.1007/s40139-014-0057-8

MYOFIBROBLAST (TATIANA KISSELEVA, SECTION EDITOR)

Strategies to Detect Hepatic Myofibroblasts in Liver Cirrhosis of Different Etiologies

Keiko Iwaisako · Kojiro Taura · Yukinori Koyama · Kenji Takemoto · Masataka Asagiri

Published online: 14 September 2014

Abstract Liver cirrhosis, a late stage of hepatic fibrosis, is an increasing cause of morbidity and mortality worldwide. Hepatic fibrosis is mainly caused by alcoholic or non-alcoholic steatohepatitis, chronic viral hepatitis, or autoimmune and biliary diseases. Myofibroblasts, which are absent from the normal liver, are differentiated from heterogeneous cell populations in response to a liver injury of any etiology and produce the extracellular matrix. Hepatic stellate cells are considered the main source of myofibroblasts. However, the origin of hepatic myofibroblasts remains unresolved, and despite considerable research, only a limited success has been achieved by existing anti-fibrotic therapies. The question remains whether these limitations are caused by lack of attention to the critical targets, the myofibroblasts derived from cells of other mesenchymal origins. Therefore, identifying the origin of myofibroblasts may provide insight into the mechanisms underlying liver fibrosis, and may lead to the development of more effective therapies. This review will examine our current strategies for detecting hepatic myofibroblasts of different origins.

K. Iwaisako (✉)
Department of Target Therapy Oncology, Kyoto University Graduate School of Medicine, 54 Kawaharacho, Shogoin, Sakyo-Ku, Kyoto 606-8507, Japan
e-mail: iwaisako@kuhp.kyoto-u.ac.jp

K. Taura · Y. Koyama · K. Takemoto
Division of Hepato-Biliary-Pancreatic and Transplant Surgery, Department of Surgery, Kyoto University Graduate School of Medicine, Kyoto 606-8507, Japan

K. Takemoto · M. Asagiri
Innovation Center for Immunoregulation and Therapeutics, Graduate School of Medicine, Kyoto University, Kyoto 606-8507, Japan

Keywords Liver cirrhosis · Hepatic fibrosis · Myofibroblasts · Hepatic stellate cells · Portal fibroblasts

Introduction

Liver cirrhosis (LC) is a major, life-threatening health problem worldwide. LC results from liver injuries of numerous different etiologies, causing hepatocyte damage, hepatic inflammation, and fibrogenesis [1]. LC can lead to the development of hepatocellular carcinoma [2]. LC is histologically characterized by increased deposition in and altered composition of the extracellular matrix (ECM) and the appearance of regenerative nodules. The destruction of the normal architecture of the liver and the loss of its functional hepatocytes prevent the liver from performing its normal detoxification, synthesis, and metabolic functions, eventually leading to portal hypertension and liver failure. From a clinical standpoint, LC is regarded as an end stage disease that leads to death, unless a liver transplant is performed [3]. However, several problems are associated with liver transplantation, such as a shortage of donors, post-transplant rejection, operative risk, and high costs.

Recently, it has become increasingly clear that hepatic fibrosis is reversible if its causative agents are successfully targeted; this has proved to be the most effective treatment for LC thus far [4]. However, the underlying causative agents are treatable only in subsets of patients with liver disease. Although there has been considerable research on liver fibrosis, there are no specific treatments for this condition. An ideal anti-fibrosis therapy would be specific for fibrogenic cells in the liver and be effective in attenuating excessive ECM deposition.